

Investigating dynamics of complex system irradiated by intense x-ray free electron laser pulses

This content has been downloaded from IOPscience. Please scroll down to see the full text.

2015 J. Phys.: Conf. Ser. 601 012006

(<http://iopscience.iop.org/1742-6596/601/1/012006>)

View [the table of contents for this issue](#), or go to the [journal homepage](#) for more

Download details:

IP Address: 131.169.95.181

This content was downloaded on 05/05/2015 at 09:06

Please note that [terms and conditions apply](#).

Investigating dynamics of complex system irradiated by intense x-ray free electron laser pulses

L Fang^{1,2}, Z Jurek^{3,4}, T Osipov¹, B F Murphy¹, R Santra^{3,4,5} and N Berrah⁶

¹ Physics Department, Western Michigan University, Kalamazoo, MI 49008 USA

² The Center for High Energy Density Science, University of Texas at Austin, Austin TX 78712 USA

³ Center for Free-Electron Laser Science, DESY, 22607 Hamburg, Germany

⁴ The Hamburg Centre for Ultrafast Imaging, 22761 Hamburg, Germany

⁵ Department of Physics, University of Hamburg, 20355 Hamburg, Germany

⁶ Physics Department, University of Connecticut, Storrs, CT 06269 USA

E-mail: Nora.berrah@uconn.edu

Abstract. We carried out experimental and theoretical investigation of the response of a complex molecule, C_{60} , to intense x-ray photon beam from a free-electron-laser. We show good agreement between the modelling and the experiment. Our model, which can be scaled well to larger systems, reveals femtosecond molecular dynamics details, at the level of atomic resolution, which are inaccessible directly by our experiments. Our results illustrate the variety of physical and chemical processes in the interaction between large molecules and intense x-ray pulses, including photoelectric effect, secondary ionization, recombination and inter-atomic Auger decays. The understanding of these processes has a broad impact on research that implements intense x-ray pulses.

1. Introduction

The recent development of intense photon sources in the x-ray regime and femtosecond time scale, allows the understanding of the fundamental response of atoms and molecules to these photon beams underpinning a broad range of research, that includes biology and chemical sciences [1]. While the investigations of the behavior of atoms and small molecules exposed to the extreme condition set by the intensity of free electron lasers (FELs) have just been launched, the exploration of larger molecules is even more nascent due to the complexity of the molecular structures and the interaction processes.

We carried out experimental and theoretical investigation on the photon interaction of a midsize molecule, C_{60} , using x-ray pulses from the Linac Coherent Light Source (LCLS) FEL. The experiment was performed at various photon beam parameters. Our theoretical model was validated based on the good agreement between the experimental and the simulation results in terms of molecular and atomic ion yields and fragment atomic kinetic energies. Our model presents various dynamical molecular ionization processes that are absent in atomic scenario. It reveals with atomic resolutions, the evolution of the molecular electronic and nuclear structure, i.e., the explosion of the molecule, and the evolution of the ionization stages and internal potentials during and after the photon-interaction. We show that the contribution of several effects, such as secondary ionization, recombination and molecular chemical bonds, are very important in comparison to atomic scenario and modeling with inclusion of selected molecular effects [2].



The dominant ionization mechanism for atoms and molecules irradiated by intense x-ray photon beams is sequential ionization - multiple sequential core-level ionization followed by subsequent Auger decay, which has been observed in atoms [3] as well as in small molecules [4]. For a large system such as C_{60} , many electrons are generated via photoionization, Auger decays and secondary ionization. Some of them leave the system, leading to a highly charged positive ion that may trap other ejected electrons. Chemical bonds of various strength between carbon atoms also play a role in determining the ionization and fragmentation pathways, adding complexity to the photon-interaction dynamics and hence, adding difficulties in predicting the final outcomes. All these processes which occur at femtosecond time scales contribute to the experimental observation, but, in the current experiment, the detailed dynamical information is lost, because we used a single pulse and the pulse duration is comparable to the time scale of the dynamical processes themselves. However, with a model validated by direct comparison with experimental quantities, we are able to take snapshots of the dynamics and therefore, gain insights into the evolution of the system, i.e. what the contribution of the various processes is.

2. Experiment and theoretical model

The experiment was performed at the atomic, molecular and optical physics (AMO) hutch of the Linac Coherent Light Source (LCLS) at SLAC National Accelerator Laboratory using the High Field Physics instrument [5]. The x-ray beam was focused to achieve a peak focal intensity of 10^{16} – 10^{18} W/cm² and crossed a collimated molecular beam of C_{60} molecules from a resistively heated oven at the focus. A magnetic bottle spectrometer was used for kinetic energy (KE) resolved ion time-of-flight spectroscopy with high collection efficiency, even at several hundred eV ion KE.

In the last decade, several theoretical models have been developed to study the evolution of samples irradiated by x-ray FEL pulses [6]. For simulation of large systems under these extreme conditions which are likely to end up in highly excited states, fully quantum mechanical methods are numerically not feasible today. In the current work, we developed a molecular dynamics (MD) model, where we utilized the XMDYN [7] tool to model finite samples irradiated by high intensity x-ray pulses. In our model, we used an atomistic description of C_{60} combined with a molecular dynamics treatment of the real space dynamics. The electronic configurations of the individual atoms/ions were tracked and utilized. Cross sections and rates for photoionization, fluorescent and Auger relaxation processes were calculated by the XATOM toolkit [7] and the Monte Carlo algorithm was implemented to describe these stochastic events. Within the model, electrons and ions are treated using classical mechanics. The fullerene-specific classical Brenner force field accounted for the chemical bonds between atoms, and the Coulomb forces for the interaction between the charged particles. The real-space evolution of the system was obtained by numerically solving the Newton equations.

For a direct comparison of experiment and theory, the actual x-ray FEL pulse properties at the interaction region must be known. Calibrations revealed that the x-ray FEL parameters can differ from the nominal values provided by LCLS, e.g. the actual pulse duration is 50–60% of the nominal value as also indicated by earlier work [3]. Our calibrations indicated that for the nominal pulse durations of 7, 20, 60, and 150 fs full width at half maximum recorded with the experimental data, actual pulse durations of 4, 13, 30, and 90 fs respectively are more appropriate. We use throughout this paper the ‘actual’ calibrated pulse durations, and we refer to these as short (4 fs), intermediate (13, 30 fs), and long pulses (90 fs).

3. Results and discussion

3.1. Comparison between experimental results and simulations – validation of a model for understanding the dynamics of large systems under extreme conditions

We measured both molecular ions of various charges and atomic ions from 1+ to up to 6+ as the outcome of the ionization by the LCLS x-ray pulses at 485 eV and 600 eV. The atomic C ions are part of the final products subsequent to the various molecular processes the effect of which was imprinted in the ion yields and KE. The FEL beam has a spatially non-homogeneous intensity distribution. According to modelling full atomic fragmentation happens at the highest intensities, while molecular fragments originate from lower fluence regions. Therefore the atomic species are our main focus in the comparison between the modeling and the experiment. We note, however, that low charge state atomic ions, in particular C^{1+} , are also formed at lower fluences. The atomic charge state distributions change when varying the x-ray beam parameters, such as the pulse energy and the pulse duration. Figure 1

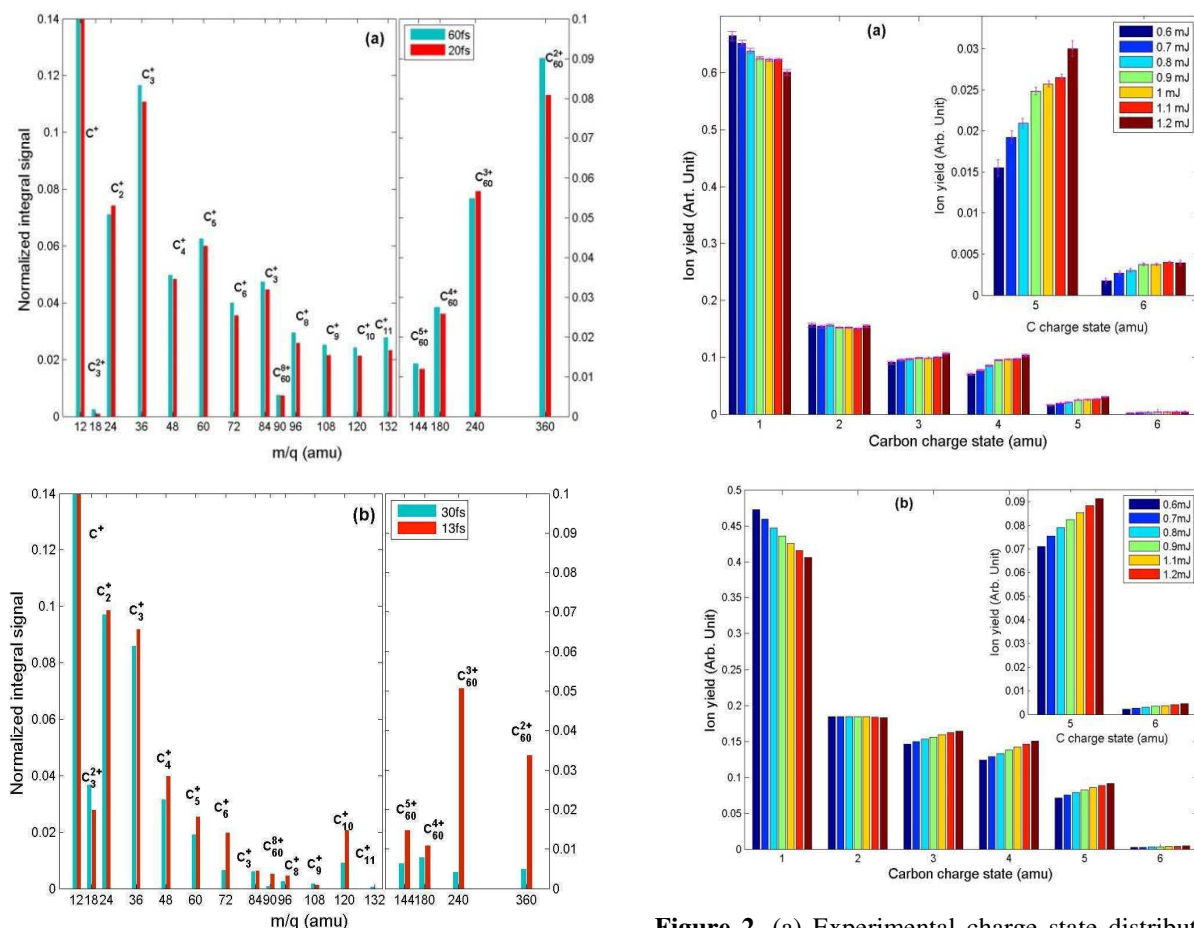


Figure 1. (a) Experimental integral signals of molecular peaks at two pulse duration. The photon energy is 600 eV; the pulse energy is 0.61 mJ. The C^+ peak is out of scale in the current plots. (b) Calculations using parameters that model best the measurements at intermediate pulse duration. The figure is adapted from [8].

Figure 2. (a) Experimental charge state distribution of atomic C ion fragments at various pulse energies and the same (long) pulse duration. The photon energy is 485 eV. (b) Calculated charge state distribution. Figure is adapted from [8]. Experimental data were obtained by direct summation of the signals by x-ray shots of particular pulse energies as shown in the legend. For each charge state, bars from left to right correspond to energies from low to high.

shows experimental (upper panel) and simulated (bottom panel) yields of various molecular ions (and atomic C^+ ion) at two different pulse durations. Though there are similar trends in the experimental and theoretical data, the appearing discrepancy indicates that there is still challenge for theory to capture fragmentation dynamics in this region. On the other hand our model successfully reproduces the observed atomic charge state distribution at various x-ray beam parameters, as seen in figure 2. Figure 2 shows experimental results (upper panel) and simulation results (bottom panel) of atomic carbon ion yields for all charge states at different pulse energies. The simulation of the pulse energy dependence of the ion yields for various charge states matches qualitatively the experimental data.

We also compare the atomic ion KE from simulations to the experimental data. Figure 3 shows the comparison between the model and experimental KE of atomic C ions generated at the high fluence part of the x-ray pulse (except that C^+ was produced at low fluence). Measured ion KE distributions show good agreement with the calculations in both mean ion energy and RMS energy spread for short and intermediate pulse durations at near constant x-ray fluence. Agreements between experiments and the simulation in various aspects validate our MD model.

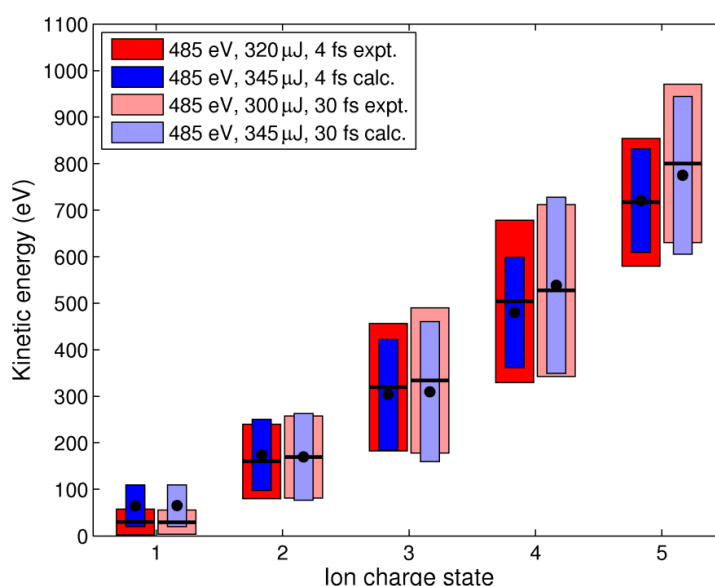


Figure 3. Fragment ion kinetic energy versus charge state. Experimental data (wide rectangles) and calculations (narrow rectangles) are displayed for short and intermediate duration pulses. Mean ion kinetic energy versus charge state is indicated by lines (experiment) and circles (simulation) at the center of each rectangle, while RMS kinetic energy width is indicated by the height of each rectangle. Pulse energy in simulation is 345 μ J compared to experimental data taken at 320 μ J (short pulses) and 300 μ J (intermediate pulses). The figure is adapted from [2].

3.2. Evolution of expanding C_{60} molecule irradiated by intense x-ray pulses

With our MD model, we simulated the electronic and nuclear dynamic evolution of expanding C_{60} molecules irradiated by LCLS, as shown in figure 4. Early in the x-ray laser pulse, due to photoionization and Auger electron emission, high energy electrons appear that can escape, leaving behind a highly charged C_{60} ion accumulating Coulomb potential energy (figure 1(a)). C_{60} starts to explode due to the increasing ion repulsion, and substantial atomic displacement (~ 10 Å) occurs within the first tens of femtoseconds (figure 4(b)(c)). As the ionic potential increases, later on during the pulse, some of the photo- and Auger electrons, together with slow electrons generated via secondary ionizations, are trapped by the increasing ionic potential, forming a nanoplasma surrounding and penetrating the remnant of the buckyball, while electrons that could escape are already at large distances (figure 4(c)). The electron nanoplasma expands with the carbon ions and a

fraction of it evaporates within nanoseconds, while others recombine forming the final detectable ionic charge states (figure 4(d)(e)).

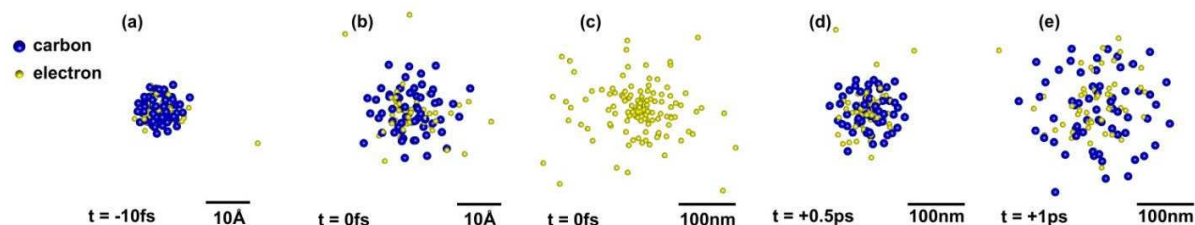


Figure 4. Simulated real space snapshots of the time evolution of a C_{60} molecule irradiated at the center of the focus of the x-ray free electron laser pulse. Spatial distribution of carbon atoms (solid dark color spheres) and electrons (solid light color spheres) are shown as a function of time at fine spatial scale (a, b) and expanded spatial scale (c, d, e). The centre of the pulse is at $t = 0$ fs and the photon energy is 600 eV with 30 fs pulse duration and 0.6 mJ pulse energy. The figure is adapted from [8].

We tracked the time evolution of the average radius of C_{60} and of the charge per C atom. Figure 5 shows the average radius of the system and the KE per atom as a function of time. At all pulse fluences used in the simulations, within the first 100 femtoseconds, the fragment ions reach their asymptotic velocity having converted most of the accumulated potential energy into kinetic energy. At higher fluences, it takes less time to reach the asymptotic velocity.

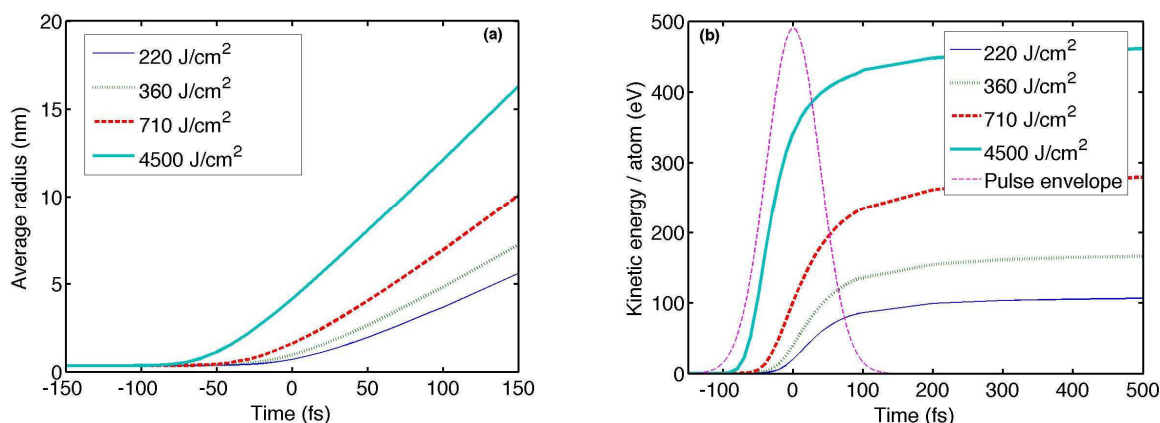


Figure 5. Calculated average molecular radius (a) and KE per atom (b) as a function of time at different pulse fluences. The photon energy used is 485 eV and the pulse duration used is 90 fs (long pulses). The molecules expand from an initial average radius of 355 pm. Fluence above 360 J cm^{-2} produces full atomic fragmentation in our calculations. Time zero corresponds to the center of the pulse. The figure is adapted from [2, 8].

3.3. Atomic vs molecular scenario – demonstrating molecular ionization mechanisms

To show the molecular effects that influence the properties of the atomic ions resulting from C_{60} ionization and fragmentation, we compare the theoretical results regarding atomic charge states using the ionization of atomic C and the ionization of C_{60} . Figure 6 shows the atomic ion yields obtained from the ionization of atomic C and for molecular C_{60} using the MD model. With the atomic model, the ion yields present an alternation pattern in the intensities between odd and even charges states till the Auger decay is not possible due to lack of valence electron at charge larger than 3. This is seen in experiments with atoms [3] where interatomic Auger decay is absent and is resultant from the photoionization and Auger event sequence that removes two electrons at a time. For molecules, this pattern breaks down, since molecular ions can fragment following various fragmentation pathways and interatomic Auger decay can occur as well. For example, dissociation of a C_2^{2+} ion leads to 2 C^+ ions. According to the results of the molecular model, we see a monotonic decrease of ion yields for

higher charge stages with the highest abundance in C^+ , in huge contrast with the result from the atomic model.

As mentioned above, the discrepancy between the results from the atomic and molecular models is partially due to electrons' redistribution during dissociation and ending up in different atoms. There are other mechanisms that are absent in atomic ionization that contribute to the final outcomes. Beside the photoionization and Auger relaxation, secondary ionization and electron recombination events take part in changing the charge states, as indicated in figure 7. We have calculated the number of ionization events associated with various ionization mechanisms using an atomic and a molecular model for long and short pulse durations (figure 7). In the case of a single C atom, since only photoionization and Auger decay contribute to ionization, as seen in figure 7(a), the final charge number equals to the total ionization event number. In the molecular model (figure 7(b)), a significant number of secondary ionization events occur. This increase of ionization events by secondary ionization is traded off to a certain degree by its resultant suppression of Auger decay, since the two mechanisms both involve valence electrons and therefore compete with each other (in figure 7 the overall suppression of Auger and photoionization events is seen for x-ray fluence over 1000 J cm^{-2} and can also be attributed to the deletion of core electrons by very intense x-ray pulses). As a result, with a similar number of photonization events, the total number of ionization events remains similar in both models. A dramatic deviation of the molecular model from the atomic one is that the final average atomic ion charge is 1-2 charges less than the average number of ionization per atom, indicating the occurrence of electron recombination that further suppresses ionization. For the short pulse, photoionization is suppressed similarly in both models due to core-electron depletion. However, in a molecule, with a short pulse a stronger attractive potential of the atomic ions can be built up that enhances electron trapping, and thus enhances recombination. Consequently, application of short pulse has a stronger effect in the suppression of ionization in molecules than in atoms, as indicated by the larger difference in the final charge number at short and at long pulses in the molecular model compared to the atomic model (figure 7). With all of the above, we conclude that for C_{60} , the high charge suppression in the ion yields is due to electron trapping followed by recombination.

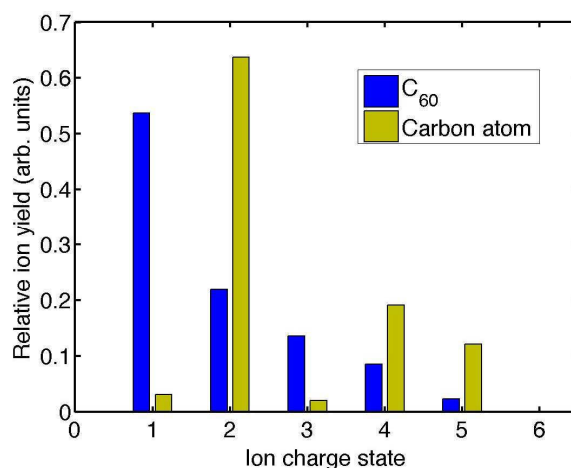


Figure 6. Theoretical ion yields for a single carbon atom and C_{60} . For this calculation the pulse duration was 30 fs, and the pulse energy was 345 μJ . The volume integrated signals were calculated using pulse parameters from the experiment. The huge discrepancy in the C^{1+} and C^{2+} yields is a direct consequence of atomic Auger (that produces C^{2+} from a neutral atom) and molecular Auger effect (that produces two C^{1+} ions from neutral ones in C_{60}), respectively. The figure is adapted from [2].

3.4. Contributions of various molecular effects in the interaction of C_{60} with intense x-rays

In addition to the various molecular dynamical processes that play distinct roles in the ionization progression, there are other molecular effects that influence the ionization, such as chemical bonds.

With our approach of adding and removing particular molecular effects in the model, we are able to determine the relative contributions of each molecular component to the final ionic outcomes. Figure 8 shows the comparison of fractional ion yields from the experiment and from the modelling with selected molecular effects included. The different degrees of discrepancy between the simulation at various conditions and the experimental data show the importance of various molecular effects in the photon interaction with C_{60} . The comparison clearly shows that i) all molecular effects are needed for the best agreement, ii) the failure of a model without any molecular effect, and iii) the importance of secondary ionization even for a midsize molecule as C_{60} . As seen in figure 8, the inclusion of the secondary ionization leads to the most significant improvement of the model to match the experimental data. Although secondary ionization has been previously reported in the case of very large Xe VdW clusters [9] and solid aluminium [10] our investigation, to the best of our knowledge, reveals for the first time significant collisional ionization *within a single molecule* exposed to intense x-rays.

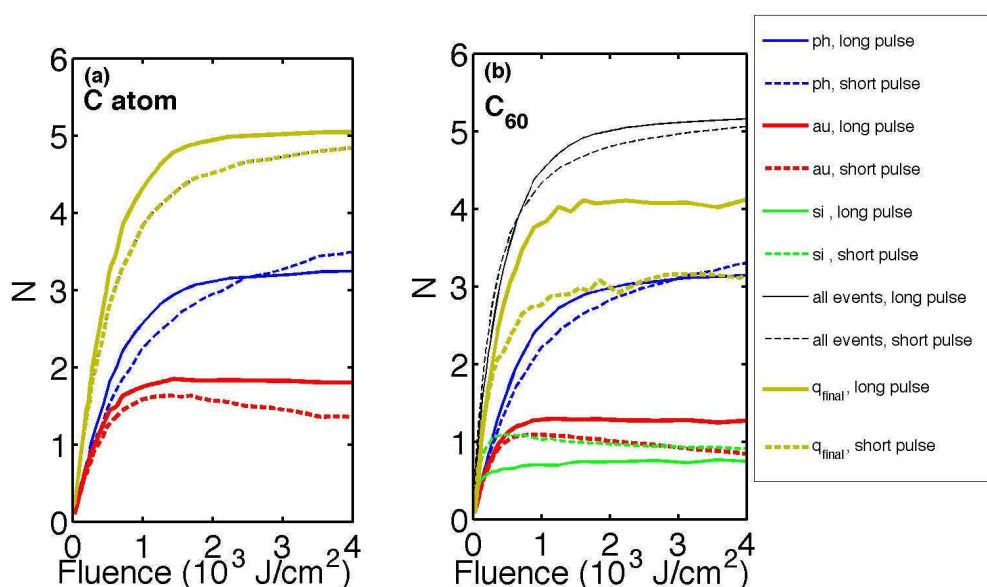


Figure 7. Comparison of atomic and molecular absorption versus volume integrated x-ray pulse peak fluence. Number of ionization events and final charge states per atom for (a) single carbon and (b) C_{60} at long and short pulse duration are shown as a function of fluence. Abbreviations: ph: photoionizations, au: Auger events, si: secondary ionization events, all: the sum of all ionization events; Q_{final} : final charge state, after recombinations in the C_{60} case. For the single carbon case there is no secondary ionization, and the “all” and “ Q_{final} ” curves overlap. The figure is adapted from [2].

Intuitively, one would expect that completely neglecting molecular bonds will always result in larger KEs, because we remove attractive binding energy from the system (in the C_{60} case it is approximately -430 eV). However, according to our model for the high fluence, long pulse cases, neglecting the molecular bonds can in fact have the opposite effect, as shown in figure 9(a). Without bonds the molecular ions can start expanding very early during the pulse with less chance to build up a concentrated high charge and in this way resulting in reduced ion KE. However, under certain conditions neglect of bonds can be reasonable. When the ionization is so fast the atoms have no chance to move before the bonds are broken, as in the case of short pulse and high fluence, the influence of the chemical bonds reduces. As shown in figure 9 for the 4 fs pulse duration case, bondless modelling yields practically the same KEs and ion yields in this regime (short pulse and high fluence), indicating that the simplification of neglecting chemical bonds in radiation damage calculations is adequate for fast ionization by x-ray beam of very high intensity.

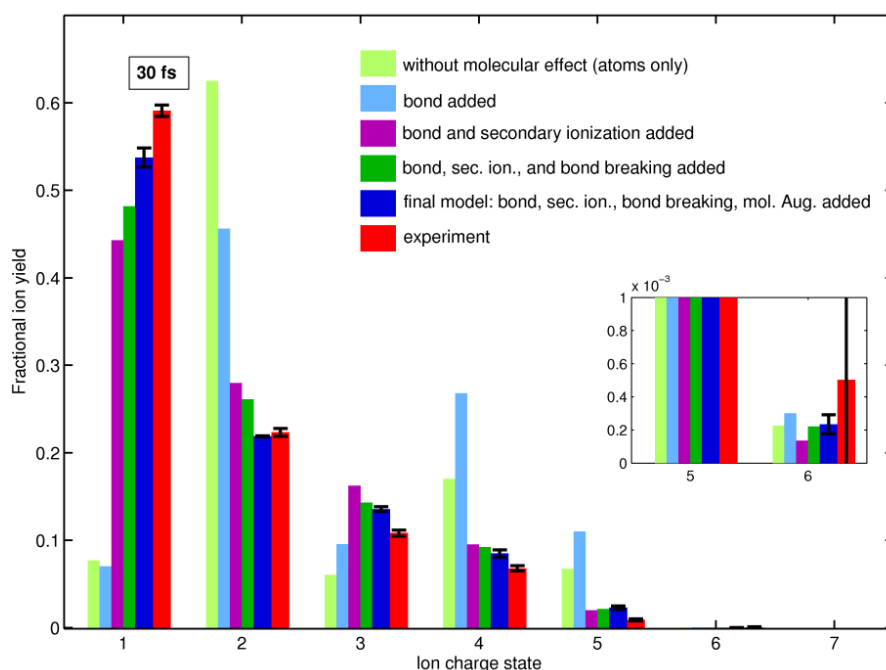


Figure 8. Importance of molecular effects reflected by the discrepancy between ion yields from experiment and from different modeling scenarios. Atomic ion yields were extracted using a model without any molecular phenomena and with an increasing number of effects until reaching the final model. Data are for the intermediate pulse duration case. Experimental data error bars are one standard deviation; modeling error bars are one standard deviation using Poisson statistics. The C^{6+} yield is near the experimental detection limit (inset). The figure is adapted from [2].

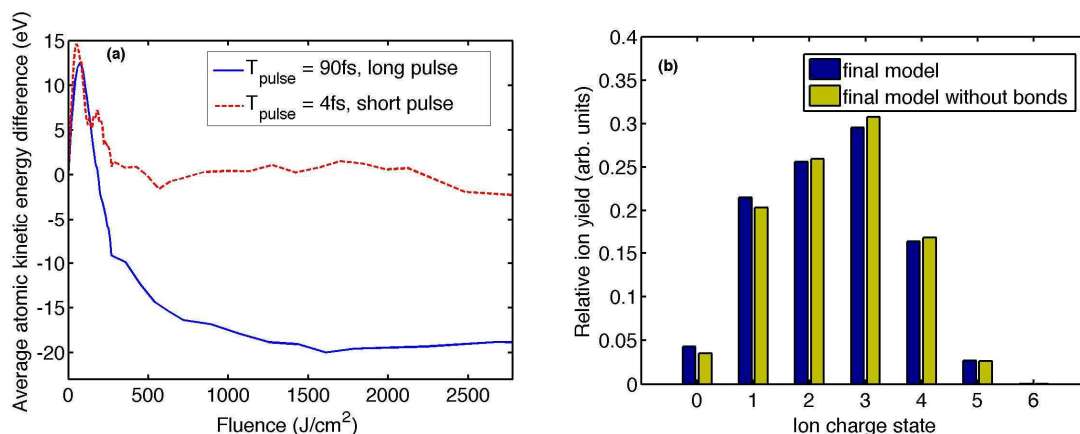


Figure 9. Modelled kinetic energy and ion charge state of atomic fragments from C_{60} as a function of fluence. The difference (a) between average atomic kinetic energies obtained from the model without bonds and that obtained from the full model ($KE^{bondless\ model} - KE^{full\ model}$) are shown for two pulse durations. Atomic ion yields (b) show agreement between the two models in the short pulse, high fluence case (in this example: photon energy is 485 eV, pulse duration 4 fs, fluence is $550\ J\ cm^{-2}$). The figure is adapted from [2].

4. Conclusion

The photo-absorption of x-rays from an FEL by a strongly bonded molecule such as C_{60} displays complex dynamics driven by various physical and chemical phenomena. With a model combining classical MD and quantum methods, we are able to investigate molecular dynamical processes and the

time evolution of the molecular system. Our model was validated by good agreement between the experimental data and the simulation results. We find that various molecular mechanisms, such as secondary ionization, electron recombination and chemical bonds, play significant roles in determining the final products. The finding of these various contributions to the ionization dynamics can be used to manipulate and control a molecular system by tuning appropriately the x-ray beam parameters. Our model provides a tool to gain insight into molecular dynamics under extreme conditions resultant from the interaction with intense FEL pulses and can be extended and used for larger molecules such as bio-systems.

Acknowledgments

This work has been supported by the Department of Energy, Office of Science, Basic Energy Sciences, Division of Chemical Sciences, Geosciences, and Biosciences, by the excellence cluster 'The Hamburg Centre for Ultrafast Imaging-Structure, Dynamics and Control of Matter at the Atomic Scale' of the Deutsche Forschungsgemeinschaft.

References

- [1] Berrah N *et al.* 2010 *J. Mod. Opt.* **57** 1015
- [2] Murphy B F *et al.* 2014 *Nature Communication* **5** 4281
- [3] Young L *et al.* 2009 *Nature* **466** 56
- [4] Fang L *et al.* 2013 *Phys. Rev. Lett.* **109** 263001
- [5] Bostedt C *et al.* 2013 *J. Phys. B: At. Mol. Opt. Phys.* **46** 164003
- [6] Neutze R *et al.* 2000 *Nature* **406** 752; Jurek Z, Faigel G and Tegze M 2004 *Eur. Phys. J. D.* **29** 217; Hau-Riege S P, London R A and Szoke A 2004 *Phys. Rev. E* **69** 051906
- [7] Jurek Z, Ziaja B and Santra R 2013 *XMDYN. Rev.* **1.0360** (CFEL, DESY); Son S-K and Santra R 2011 *XATOM*—an integrated toolkit for x-ray and atomic physics (CFEL, DESY)
- [8] Berrah N *et al.* *Faraday Discussions* 2014 DOI: 10.1039/C4FD00015C
- [9] Thomas H *et al.* 2012 *Phys. Rev. Lett.* **108** 133401
- [10] Ciricosta O *et al.* 2012 *Phys. Rev. Lett.* **109** 065002